

Backward waves in magnetoelectrically chiral media: Propagation, impedance, and negative refraction

Cheng-Wei Qiu,^{1,2} Hai-Ying Yao,¹ Le-Wei Li,^{1,*} Saïd Zouhdi,² and Tat-Soon Yeo¹

¹*Department of Electrical and Computer Engineering, National University of Singapore, Kent Ridge, Singapore 119260*

²*Laboratoire de Génie Electrique de Paris, CNRS, Ecole Supérieure D'Électricité, Plateau de Moulon 91192, Gif-Sur-Yvette Cedex, France*

(Received 18 September 2006; published 30 April 2007)

Magnetolectrically chiral media are studied in this paper as potential materials to realize double negative materials and negative refractive characteristics. The behaviors of the negative refractive index, the backward eigenwaves, and the impedance of these eigenmodes of this particular type of chiral media are examined in detail. We consider longitudinal and transverse propagation separately. Among the wave numbers obtained, we find that two of them are backward propagating waves in certain frequency bands. The helicity and polarization states are shown. We further study the impedance of these backward eigenmodes, which have potential applications in impedance matching, subwavelength resonator cavities and high-directivity antennas. Due to the off-diagonal gyrotropic parameters, a negative refractive index can be achieved when the material parameters and frequency are properly chosen. A study of the zero index of refraction for magnetoelectrically chiral media is carried out, and potential applications are proposed.

DOI: [10.1103/PhysRevB.75.155120](https://doi.org/10.1103/PhysRevB.75.155120)

PACS number(s): 78.20.Ek, 42.25.Gy, 42.25.Bs, 33.55.Ad

I. INTRODUCTION

Recently, metamaterials (with simultaneously negative permittivity and permeability in a frequency band), as a kind of novel artificial material, have received considerable interest within the scientific community. Metamaterials possess a lot of exotic properties, such as a negative index of refraction, reversal Doppler shift and Vavilov-Cerenkov effect,¹ a reversed circular Bragg phenomenon,² and the superlens.³ Although perfect lenses are difficult to realize, subwavelength imaging can still be achieved when the lens is slightly lossy.⁴ Other potential applications of metamaterials have been explored, including periodical dipole arrays,⁵ leaky wave antennas,⁶ and subwavelength cavity resonators.⁷ Since the negative-refractive-index materials were experimentally verified by Shelby *et al.*⁸ and Houck *et al.*,⁹ some researchers have further studied tensor-parameter retrieval using quasi-static Lorentz theory,¹⁰ *S*-parameter retrieval using plane wave incidence,¹¹ and constitutive relation retrieval using the transmission line method.^{12–14} In addition, some new structures^{15,16} have been proposed. As for the realization of negative-refractive-index materials, there are several approaches, including transmission line grids or composite structures,¹⁷ optically resonant materials,¹⁸ uniaxially anisotropic structures,¹⁹ and photonic crystals.²⁰

In one recent paper,²¹ negative refraction was studied in gyroplasma chiral media (with magnetoelectric coupling present only in electric displacement), where the spatial dispersion approach was applied in the analysis of a chiral medium's response in the vicinity of the longitudinal frequency. More recently, the Green's dyadics and some potential applications of negative refraction in the quantum vacuum have been studied,²² and a study on the constitutive relations of magnetoelectric materials has also been carried out.²³ Unlike the work reported above, in this paper, we will focus on the electromagnetic propagation properties of backward waves, impedance matching, and the realization of equivalent per-

mittivity and/or permeability associated with the negative refraction of backward waves in magnetoelectrically chiral media. We will also discuss the possibility of achieving zero refractive index with a positive wave impedance, and its applications. As is known, little attention has been paid so far to possible backward wave propagation in chiral media since it is believed that both of the two eigenwaves are forward propagating due to a parameter restriction.²⁴ Actually, it was proved by Tretyakov *et al.*²⁵ that this restriction is not necessary, and some other studies also show that backward waves can propagate in chiral media.^{26,27} Note that, in nature, the chiral parameter is not big for chiral media. Hence, a chiral medium with small permittivity or permeability favors the realization of backward waves and negative refraction. Chiral nihility is a special case which holds only near the resonant frequency. Therefore, the main contribution of this paper are as follows. (i) A negative index of refraction in a magnetoelectrically chiral medium can be realized with fewer restrictions (e.g., a chiral medium requires a small permittivity at a working frequency so as to obtain a negative refractive index). (ii) Two backward eigenwaves are found due to the effects of the gyroelectric and gyromagnetic parameters. (iii) All parameters in the permittivity and permeability tensors as well as the chirality admittance can be positive when negative refraction occurs. These three points represent also the advantages of the presently considered magnetoelectrically chiral materials over normal chiral or bi-isotropic materials. Furthermore, we also propose the physical conditions for realizing backward waves and demonstrate how to fabricate superlenses by the use of magnetoelectrically chiral materials, matching the impedances and choosing an appropriate frequency. In addition, it is found that a zero refractive index associated with a positive impedance can be achieved, which will have great potential applications in antenna directivity enhancement and phase conservation.

II. BACKWARD PROPAGATING WAVES AND THEIR IMPEDANCE

The description of magnetoelectrically chiral media can be obtained by generalizing the scalar constitutive relations for isotropic chiral media:

$$\mathbf{D} = \bar{\boldsymbol{\epsilon}} \cdot \mathbf{E} + i\xi_c \mathbf{B}, \quad (1)$$

$$\mathbf{H} = i\xi_c \mathbf{E} + \bar{\boldsymbol{\mu}}^{-1} \cdot \mathbf{B}, \quad (2)$$

where ξ_c denotes the chirality admittance and

$$\bar{\boldsymbol{\epsilon}} = \begin{bmatrix} \epsilon & -ig & 0 \\ ig & \epsilon & 0 \\ 0 & 0 & \epsilon_z \end{bmatrix}, \quad (3)$$

$$\bar{\boldsymbol{\mu}} = \begin{bmatrix} \mu & -iw & 0 \\ iw & \mu & 0 \\ 0 & 0 & \mu_z \end{bmatrix}. \quad (4)$$

The generalized medium studied in this paper can be reduced to (i) a chiroplasma consisting of chiral objects embedded in a magnetically biased plasma, or (ii) a chiroferrite obtained by immersing chiral objects into magnetically biased ferrite.²⁸ At this moment, there has been no report about fabricated materials with these kinds of gyrotropies in both permittivity and permeability. The most recent progress in manufacturing technology, however, suggests that this kind of material will be very likely realized in a short time frame from various potential composites, especially when nanoscaled particles, ferrites, and plasmas are mixed together using advanced molding, design, and fabrication techniques. Some new fabrication facilities available elsewhere in the world have made it possible to manufacture such complex composites by adopting some new molding and filling techniques in the optical frequency region. Thus, the appearance of such media is greatly anticipated, and theoretical study always goes ahead of experiments for design guidance. Nevertheless, generality in such media can also be useful, because the present theorem can be directly applied to either the chiroplasma or the chiroferrite case. These two subsets are still of great potential, as compared to conventional plasma or ferrites, due to the existence of magnetoelectric coupling.

The constitutive relations of the material discussed in this paper are of Boys-Post type. It is also worth noting that our material is a generalization of gyrotropic (chiral) media without the assumption of $\mathbf{H}:\mathbf{H}=\mathbf{B}$.²⁹ Throughout the paper, the time dependence $e^{-i\omega t}$ is suppressed and the time-harmonic Maxwell equations in the source-free case will be used:

$$\nabla \times \mathbf{E} = i\omega \mathbf{B}, \quad (5)$$

$$\nabla \times \mathbf{H} = -i\omega \mathbf{D}. \quad (6)$$

Substituting the constitutive relations into above equations, we have

$$\nabla \times [\bar{\boldsymbol{\alpha}} \cdot \nabla \times \mathbf{E}] - 2\omega\xi_c \nabla \times \mathbf{E} - \omega^2 \bar{\boldsymbol{\epsilon}} \cdot \mathbf{E} = 0, \quad (7)$$

where

$$\bar{\boldsymbol{\alpha}} = \bar{\boldsymbol{\mu}}^{-1} = \begin{bmatrix} \alpha_t & -\alpha_a & 0 \\ \alpha_a & \alpha_t & 0 \\ 0 & 0 & \alpha_z \end{bmatrix} \quad (8)$$

and

$$\alpha_t = \frac{\mu}{\mu^2 - w^2}, \quad (9)$$

$$\alpha_a = -i \frac{w}{\mu^2 - w^2}, \quad (10)$$

$$\alpha_z = \frac{1}{\mu_z}. \quad (11)$$

A. Wave propagation inside a magnetoelectrically chiral medium

Assume that a plane wave is propagating along the z axis inside a magnetoelectrically chiral medium and its form is given by $e^{i(\mathbf{k}\cdot\mathbf{r}-\omega t)}$. There are two approaches for obtaining the eigenmodes and wave numbers, namely, (i) starting from Eq. (7) and obtaining the nontrivial solutions of the wave number matrix, and (ii) starting from the constitutive relations directly, listing all the relations of the field components, and solving the final equation consisting of wave numbers and parameters only. Here we choose the second, which is less cumbersome and gives more insight into the physical properties of the electromagnetic waves inside the medium.

If the plane waves are confined to propagate along the z axis, we have E_z and H_z equal to zero for the nontrivial solutions. Since \mathbf{E} and \mathbf{H} have only transverse components and the parameter is in gyrotropic form, D_z and B_z vanish. Thus we have the following relations:

$$\begin{bmatrix} H_x \\ H_y \end{bmatrix} = i\xi_c \begin{bmatrix} E_x \\ E_y \end{bmatrix} + \begin{bmatrix} \alpha_t B_x - \alpha_a B_y \\ \alpha_a B_x + \alpha_t B_y \end{bmatrix}, \quad (12)$$

$$\begin{bmatrix} D_x \\ D_y \end{bmatrix} = \begin{bmatrix} \epsilon E_x - ig E_y \\ ig E_x + \epsilon E_y \end{bmatrix} + i\xi_c \begin{bmatrix} B_x \\ B_y \end{bmatrix}. \quad (13)$$

For plane wave propagation, we can further put $\nabla = i\mathbf{k}$, which results in the relations of the Maxwell equations as follows:

$$\begin{bmatrix} -k_z E_y \\ k_z E_x \end{bmatrix} = \omega \begin{bmatrix} B_x \\ B_y \end{bmatrix}, \quad (14)$$

$$\begin{bmatrix} k_z H_y \\ -k_z H_x \end{bmatrix} = \omega \begin{bmatrix} D_x \\ D_y \end{bmatrix}. \quad (15)$$

From Eqs. (12)–(15), we finally arrive at two equations (lengthy intermediate steps have been suppressed):

$$\left(\frac{k_z}{\omega} \alpha_t - \frac{\omega}{k_z} \epsilon \right) E_y = i \left(2\xi_c + \frac{\omega}{k_z} g + \frac{k_z}{\omega} \sigma \right) E_x, \quad (16)$$

$$i \left(2\xi_c + \frac{\omega}{k_z} g + \frac{k_z}{\omega} \sigma \right) E_y = \left(\frac{\omega}{k_z} \epsilon - \frac{k_z}{\omega} \alpha_t \right) E_x, \quad (17)$$

where $\sigma = w/(\mu^2 - w^2)$.

In view of Eqs. (16) and (17), we can get four roots of the wave numbers. To give more physical insight into those four roots, we reorganize them by taking into account the direction of energy propagation and the polarized states:

$$k_{p\pm} = \omega \frac{\pm \xi_c + \sqrt{\xi_c^2 + (\alpha_t \mp \sigma)(\epsilon \pm g)}}{\alpha_t \mp \sigma}, \quad (18)$$

$$k_{a\pm} = \omega \frac{\mp \xi_c - \sqrt{\xi_c^2 + (\alpha_t \pm \sigma)(\epsilon \mp g)}}{\alpha_t \pm \sigma}, \quad (19)$$

where p and a represent the parallel and antiparallel direction of energy flow (i.e., the real part of the Poynting's vector) and the \pm signs refer to right-circular polarization (RCP) and left-circular polarization (LCP), respectively. One should note that the material in this paper is a generalization of Landau's model²⁹ of Boys-Post type instead of using the Tellegen relations.³⁰ Note that k_{p-} and k_{a-} could represent the wave numbers for backward eigenwaves under some situations, which will be discussed in detail later.

If we assume that the plane waves are propagating transversely, we can rewrite Eq. (7) as follows by inserting $\mathbf{E} = E_0 e^{i(k_x \hat{x} + k_y \hat{y})}$ into Eq. (7):

$$\mathbf{k}_t \times [\bar{\boldsymbol{\alpha}} \cdot (\mathbf{k}_t \times \mathbf{E}_0)] + 2i\omega \xi_c \mathbf{k}_t \times \mathbf{E}_0 + \omega^2 \bar{\boldsymbol{\epsilon}} \cdot \mathbf{E}_0 = 0, \quad (20)$$

where the transverse wave number $\mathbf{k}_t = k_x \hat{x} + k_y \hat{y}$.

Then we put the above equation into a matrix form, with one column of field components and another 3×3 matrix. When we try to get the nontrivial solutions as was done in Eq. (7), we find it impossible to simultaneously solve explicitly for k_x and k_y . Instead, we can solve for the magnitude of the transverse wave vector $k_t = \sqrt{k_x^2 + k_y^2}$, which leads to

$$k_t^4 - \omega^2 (\epsilon_v \mu_z + \epsilon_z / \alpha_t + 4\xi_c^2 \mu_z / \alpha_t) k_t^2 + \omega^4 \epsilon_v \epsilon_z \mu_z / \alpha_t = 0, \quad (21)$$

where ϵ_v [i.e., $(\epsilon^2 - g^2) / \epsilon$] and $1 / \alpha_t$ are the Voigt permittivity and permeability, respectively. Finally, we arrive at

$$k_{t\pm} = \frac{\omega}{2} \left[\sqrt{(\sqrt{\epsilon_v \mu_z} + \sqrt{\epsilon_z / \alpha_t})^2 + 4\xi_c^2 \mu_z / \alpha_t} \pm \sqrt{(\sqrt{\epsilon_v \mu_z} - \sqrt{\epsilon_z / \alpha_t})^2 + 4\xi_c^2 \mu_z / \alpha_t} \right]. \quad (22)$$

Due to the rotational symmetry in the transverse plane at $z = 0$, the magnitude of the wave vector \mathbf{k}_t can be obtained by setting the determinant of the Helmholtz equation [i.e., Eq. (20)] to zero. This shows that the magnetoelectrically chiral medium favors two elliptically polarized eigenwaves with the coefficients $k_{t\pm}$.

B. Wave impedance

As mentioned previously, one parallel LCP (i.e., k_{p-}) and one antiparallel LCP (i.e., k_{a-}) can be backward propagating with opposite directions of phase and energy velocity. The directions of the energy velocities are identical with those of the Poynting vectors, which can be verified directly from the Maxwell equations together with the constitutive relations:

$$\mathbf{S}_{p+} = \hat{z} \frac{|\mathbf{E}_0|^2}{2\eta_1}, \quad (23)$$

$$\mathbf{S}_{a-} = -\hat{z} \frac{|\mathbf{E}_0|^2}{2\eta_1}, \quad (24)$$

$$\mathbf{S}_{p-} = \hat{z} \frac{|\mathbf{E}_0|^2}{2\eta_2}, \quad (25)$$

$$\mathbf{S}_{a+} = -\hat{z} \frac{|\mathbf{E}_0|^2}{2\eta_2}, \quad (26)$$

where η_1 and η_2 denote the wave impedances of the positive and negative helicities, respectively.

In view of the above equations, the z -axis component of the Poynting vector can be shown as

$$S_z = \frac{1}{2} [E_x H_y^* - E_y H_x^*] \quad (27)$$

where the transverse magnetic fields can be obtained from Eqs. (12)–(15):

$$\begin{bmatrix} H_x \\ H_y \end{bmatrix} = \begin{bmatrix} i \left(\xi_c + \frac{k_z}{\omega} \sigma \right) E_x - \frac{k_z}{\omega} \alpha_t E_y \\ i \left(\xi_c + \frac{k_z}{\omega} \sigma \right) E_y + \frac{k_z}{\omega} \alpha_t E_x \end{bmatrix}. \quad (28)$$

Before we can solve for η_1 and η_2 , one condition should be noted, derived from Eqs. (16) and (17),

$$\left(2\xi_c + \frac{\omega}{k_z} g + \frac{k_z}{\omega} \sigma \right)^2 = \left(\frac{\omega}{k_z} \epsilon - \frac{k_z}{\omega} \alpha_t \right)^2. \quad (29)$$

Substituting Eq. (28) into Eq. (27) with the aid of the solution in Eq. (29), we finally obtain

$$\eta_1 = \frac{1}{\sqrt{\xi_c^2 + (\alpha_t - \sigma)(\epsilon + g)}} = \frac{1}{\sqrt{\xi_c^2 + \frac{\epsilon + g}{\mu + w}}}, \quad (30)$$

$$\eta_2 = \frac{1}{\sqrt{\xi_c^2 + (\alpha_t + \sigma)(\epsilon - g)}} = \frac{1}{\sqrt{\xi_c^2 + \frac{\epsilon - g}{\mu - w}}}. \quad (31)$$

Alternatively, by applying the Beltrami fields,³¹ $\boldsymbol{\epsilon}_\pm$ and $\boldsymbol{\mu}_\pm$ of the eigenmodes can also be obtained as

$$\boldsymbol{\epsilon}_\pm = \sqrt{\xi_c^2 + \frac{\epsilon \pm g}{\mu \pm w}} \{ \pm \xi_c (\boldsymbol{\mu} \pm w) + \sqrt{[\xi_c (\boldsymbol{\mu} \pm w)]^2 + (\epsilon \pm g)(\boldsymbol{\mu} \pm w)} \}, \quad (32)$$

$$\boldsymbol{\mu}_\pm = \sqrt{\frac{\mu \pm w}{\xi_c^2 (\boldsymbol{\mu} \pm w) + \epsilon \pm g}} \{ \pm \xi_c (\boldsymbol{\mu} \pm w) + \sqrt{[\xi_c (\boldsymbol{\mu} \pm w)]^2 + (\epsilon \pm g)(\boldsymbol{\mu} \pm w)} \}. \quad (33)$$

Thus, the wave impedances of those eigenmodes can be veri-

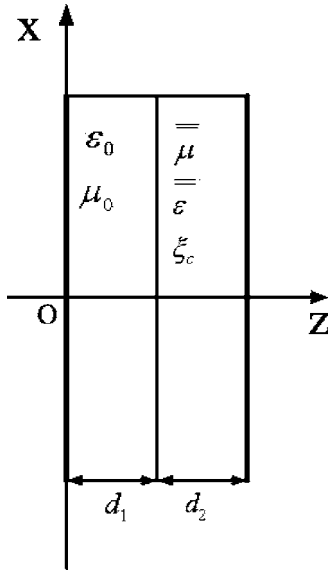


FIG. 1. Compact resonator formed by a two-layer structure consisting of air and magnetoelectrically chiral medium backed by two ideally conducting planes.

fied by using $\eta_{\pm} = \sqrt{\mu_{\pm}/\epsilon_{\pm}}$, which agree with results for η_1 and η_2 , respectively.

These findings are of importance in phase compensation and compact resonators,⁷ since good impedance matching can be achieved at the interface between a magnetoelectrically chiral slab and the adjacent spaces. Note that the elements in the permittivity and permeability tensors involve frequency, plasma frequency, electron gyrofrequency, gyromagnetic response frequency, and saturation magnetization frequency,^{32,33} and the realization of a backward wave depends on the frequency selection. Within certain frequency ranges, k_{p-} and k_{a-} could be the wave numbers of a backward wave simultaneously, or only one of them might be. Configurations of conventional and subwavelength cavity resonators are proposed using magnetoelectrically chiral slabs, when the working frequency is properly chosen to arrive at a negative refractive index.

In Fig. 1, it can be seen that, if a plane wave propagates in the direction perpendicular to the interfaces at a certain frequency range, its phase is increased in the conventional medium and can be decreased by the magnetoelectrically chiral medium. This falls into the backward wave region. It is noted that the backward eigenmodes possess two impedances. Hence, by properly controlling the parameters and the external biased fields, $\eta_+ = \eta_0$ or $\eta_- = \eta_0$ can be chosen to match the wave impedance η_0 of the air, which means two kinds of cavity resonator can be created as shown in Figs. 2 and 3.

The resonance condition for a cavity takes the form⁷

$$\frac{n_2}{\mu_2} \tan(n_1 k_0 d_1) + \frac{n_1}{\mu_1} \tan(n_2 k_0 d_2) = 0, \quad (34)$$

where the subscripts 1 and 2 correspond to the layers on the left- and right-hand sides, respectively. For the case shown in Fig. 2 when η_+ is matched, it turns out to be a conventional cavity resonator, and thus Eq. (34) becomes

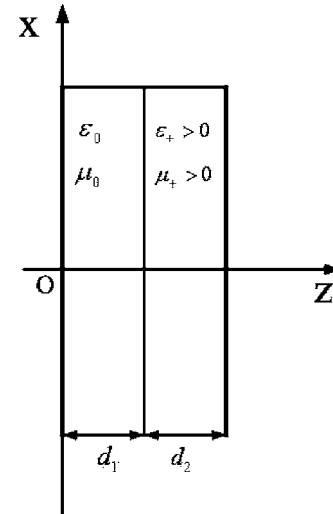


FIG. 2. Configuration of one-dimensional (1D) conventional cavity resonator.

$$n_+ d_2 + d_1 = \frac{m}{2} \lambda_0, \quad m = 0, 1, 2, \dots, \quad (35)$$

where λ_0 is the wavelength in the air.

Of particular and practical interest is the case of subwavelength cavity resonators, in which the arguments in the tangential functions can be assumed small. If η_- is matched, the resonant condition in Eq. (34) is reduced to

$$\frac{d_1}{d_2} \cong \frac{|\mu_-|}{|\mu_0|}. \quad (36)$$

It can be observed that it is not necessary to satisfy the above condition to have simultaneously negative permittivity and permeability, since only the first term in the Taylor expansion in the tangent function is kept for a thin layer on metal surfaces. The definition of n_{\pm} will be given in the following section.

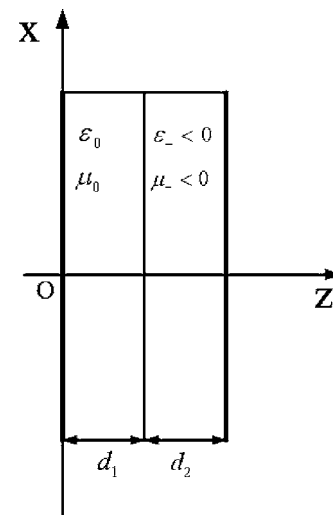


FIG. 3. Configuration of 1D subwavelength cavity resonator.

TABLE I. Helicity and polarization states of k_{p-} and k_{a-} in three cases, under the conditions of $|w| < \mu$ and $\xi_c > 0$.

	$g < -\epsilon$		$-\epsilon < g < \epsilon$		$g > \epsilon$	
	Helicity	Polarization	Helicity	Polarization	Helicity	Polarization
k_{p-}	\ominus	LCP	\ominus	LCP	\ominus^a	RCP ^a
k_{a-}	\oplus^a	RCP ^a	\oplus	LCP	\oplus	LCP
ω	$(0, \omega_{c1})$			(ω_g, ω_{c2})		

^aBackward wave regions.

III. NEGATIVE REFRACTION

k_{p-} and k_{a-} are of particular interest since they will represent the properties of backward waves under specific cases as shown in Table I. The quantities ϵ and g are given in Ref. 32 as follows:

$$\epsilon = \epsilon_0 \left(1 - \frac{\omega_p^2 (\omega + i\omega_{eff})}{\omega [(\omega + i\omega_{eff})^2 - \omega_g^2]} \right), \quad (37)$$

$$g = \epsilon_0 \frac{\omega_p^2 \omega_g}{\omega [(\omega + i\omega_{eff})^2 - \omega_g^2]}, \quad (38)$$

where ω_p , ω_g , and ω_{eff} are the plasma frequency, electron gyrofrequency, and collision frequency of the electrons, respectively.

It should also be noted that the positive (negative) helicity is defined as right-(left-)handedness to the positive (negative) z axis. The helicity and polarized states can be found by inserting Eqs. (18) and (19) into Eq. (7). When k_{p-} or k_{a-} becomes a backward wave, the handedness changes.

A collisionless case is considered here (i.e., $\omega_{eff} = 0$). First we introduce two quantities

$$\omega_{c1} = \frac{1}{2} (-\omega_g + \sqrt{\omega_g^2 + 4\omega_p^2}), \quad (39)$$

$$\omega_{c2} = \frac{1}{2} (\omega_g + \sqrt{\omega_g^2 + 4\omega_p^2}). \quad (40)$$

As shown in Table I, in order to realize the backward eigenmode k_{a-} , we can see that $\epsilon + g < 0$ should be satisfied (i.e., $0 < \omega < \omega_{c1}$ should hold). To form the backward eigenmode k_{p-} , $g > \epsilon$, which means $\omega_g < \omega < \omega_{c2}$. Note that if

$$\omega_p < \sqrt{2}\omega_g$$

is satisfied, there is no overlapping of the two intervals regarding the frequency ω . If we choose

$$\omega_p > \sqrt{2}\omega_g,$$

then both k_{p-} and k_{a-} are backward wave numbers, and two impedances will be present in any one layer of a slab in Fig. 1. In that case, it would be impossible to match those two impedances simultaneously at the material-air interface. However, we can choose one impedance equal to that of air, and correspondingly the backward wave associated with that impedance can propagate through the slabs as shown in Figs. 2 and 3. From the definitions given below:

$$\omega_p^2 = \frac{N_e e^2}{m \epsilon_0}, \quad (41)$$

$$\omega_g = \frac{e}{m_e} B_{dc}, \quad (42)$$

where the subscript dc represents the dc electromagnetic field applied to induce the gyrotropy in both the permittivity and permeability tensors. It can be seen that nonoverlapping or overlapping can be achieved by adjusting the number of electrons or the dc field. For simplicity, we can further split the field into two parts as

$$B_{dc} = \mu_0 (H_{dc} + M_{dc}), \quad (43)$$

where M denotes the magnetic moment in the whole volume occupied by a magnetoelectrically chiral material and the H field has taken into account the demagnetizing field. Then the permeability tensor can be characterized as³³

$$\mu = \mu_0 \left(1 - \frac{\omega_0 \omega_M}{\omega^2 - \omega_0^2} \right), \quad (44)$$

$$w = \frac{\omega \omega_M}{\omega^2 - \omega_0^2}, \quad (45)$$

where

$$\omega_0 = \frac{e}{m_e} \mu_0 H_{dc}, \quad (46)$$

$$\omega_M = \frac{e}{m_e} \mu_0 M_{dc}. \quad (47)$$

Therefore, it can be shown that the restriction $|w| < \mu$ (as stated in Table I) can be maintained by choosing a proper external dc magnetic field and number of electrons.

With the conditions clearly stated, the negative refractive indices of a magnetoelectrically chiral medium can be obtained, which are of particular interest. Taking into account Eqs. (18) and (19), for the respective polarization states and helicities, we can finally obtain the two refractive indices for these backward eigenwaves:

$$n_{\pm} = \frac{c_0}{(\alpha_t \mp \sigma)} \left[\sqrt{\xi_c^2 + (\alpha_t \mp \sigma)(\epsilon \pm g)} - \xi_c \right] \quad (48)$$

where the plus and minus signs refer to k_{a-} and k_{p-} , respectively.

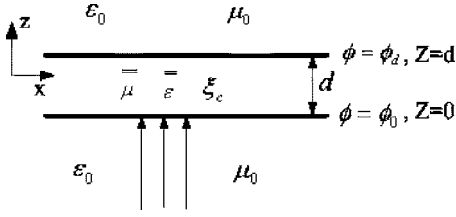


FIG. 4. Magnetoelectrically chiral slab with $n=0$ and phase conservation.

It can be seen that n_+ will be negative when $g < -\epsilon$ and n_- will possess a minus sign when $g > \epsilon$ (which means that a backward wave propagates in such a medium). Equation (48) also shows that a negative refractive index may easily be achieved even if the chirality admittance ξ_c is very small. Note that we can use all positive parameters (i.e., ϵ , g , μ , w , and ξ_c) to achieve a negative index of refraction (i.e., n_-). In addition, $g > \epsilon$ can be realized with some advanced technology in future based on the theory of off-diagonal parameter amplification in artificially gyrotropic media.³⁴

In what follows, we analyze Eq. (48) in detail to give an overview of the possibility of backward waves.

We can further rewrite Eq. (48) as

$$n_{\pm} = c_0 [\sqrt{(\mu \pm w)^2 \xi_c^2 + (\mu \pm w)(\epsilon \pm g)} - (\mu \pm w) \xi_c]. \quad (49)$$

It is found that negative refractive indices may be easily achieved if $\epsilon \pm g < 0$, and it has been pointed out how the frequency should be selected so as to give rise to negative refractive indices in Fig. 1. The case of $n_{\pm} = 0$ turns out to be of particular interest (i.e., the case $\epsilon \pm g = 0$). It follows that this case can be realized at two specific frequencies as given below:

$$\omega_1 = -\frac{\omega_g}{2} + \sqrt{\left(\frac{\omega_g}{2}\right)^2 + \omega_p^2}, \quad (50)$$

$$\omega_2 = \frac{\omega_g}{2} + \sqrt{\left(\frac{\omega_g}{2}\right)^2 + \omega_p^2}. \quad (51)$$

$\omega = \omega_1$ and $\omega = \omega_2$ lead to $\epsilon + g = 0$ and $\epsilon - g = 0$, respectively.

Therefore this can create an equivalent cover for patch antennas (see Fig. 4) with zero refractive index and a positive wave impedance $1/\xi_c$, comprised of a magnetoelectrically chiral medium. Only normally incident waves are transmitted into the slab, and the phases in any plane between $z = 0$ and $z = d$ will remain unchanged. Alternatively, as shown in Fig. 5, if some sources are placed in a substrate made from a magnetoelectrically chiral slab with $n=0$ and finite impedance, all the transmitted waves will be perpendicular to the upper surface no matter what the form of the source.

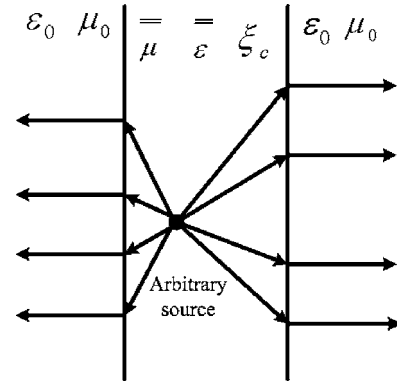


FIG. 5. Special substrate made from magnetoelectrically chiral slab with zero refractive index but finite impedance.

Hence, a magnetoelectrically chiral slab may be used as a radome of antennas, which will greatly enhance the directivity of the antennas. No reflected waves interfere with the antennas if impedance matching at the material-air interface has been done. In addition, the existence of slab has no influence on the phase of the propagating waves.

In a word, magnetoelectrically chiral media provide us a very exciting new opportunity to realize negative refraction, backward wave propagation, and other promising potential applications.

IV. CONCLUSION

In this paper, we studied important electromagnetic properties of magnetoelectrically chiral media due to their significant potential in the realization of negative-refractive-index materials. The longitudinal and transverse wave propagation in a magnetoelectrically chiral medium are considered, and properties of these eigenmodes such as helicity and polarization are fully examined in order to find the backward waves. The impedances for all eigenmodes, including the backward eigenmodes, are derived and studied. It is also found that the magnetoelectrically chiral material can be utilized to achieve negative refraction and to fabricate subwavelength cavities. For these purposes, impedance matching, gyrotropic parameter effects, and working frequency selection have been discussed. In addition, we show that a zero-refractive-index material can be achieved in such a magnetoelectrically chiral material; its characteristics and potential applications are studied.

ACKNOWLEDGMENTS

The authors are grateful for support from the SUMMA Foundation, U.S.A., and a joint project supported by the France-Singapore ‘‘Merlion Project.’’

- *FAX: (+65) 6779 1103. Email address: LWLi@nus.edu.sg; http://www.ece.nus.edu.sg/lwli
- ¹V. G. Vesalago, *Sov. Phys. Usp.* **10**, 509 (1968).
 - ²A. Lakhtakia, *Opt. Express* **11**, 716 (2003).
 - ³J. B. Pendry, *Phys. Rev. Lett.* **85**, 3966 (2000).
 - ⁴D. R. Smith, D. Schurig, M. Rosenbluth, S. Schultz, S. A. Ramakrishna, and J. B. Pendry, *Appl. Phys. Lett.* **82**, 1506 (2003).
 - ⁵G. Goussetis, A. P. Feresidis, and J. C. Vardaxoglou, *IEE Proc., Part H: Microwaves, Antennas Propag.* **152**, 251 (2005).
 - ⁶L. Liu, C. Caloz, and T. Itoh, *Electron. Lett.* **38**, 1414 (2002).
 - ⁷N. Engheta, *IEEE Antennas Wireless Propag. Lett.* **1**, 10 (2002).
 - ⁸R. A. Shelby, D. R. Smith, and S. Schultz, *Science* **292**, 77 (2001).
 - ⁹A. A. Houck, J. B. Brock, and I. L. Chuang, *Phys. Rev. Lett.* **90**, 137401 (2003).
 - ¹⁰A. Ishimaru, S. W. Lee, Y. Kuga, and V. Jandhyala, *IEEE Trans. Antennas Propag.* **51**, 2550 (2003).
 - ¹¹X. Chen, B. I. Wu, J. A. Kong, and T. M. Grzegorzczuk, *Phys. Rev. E* **71**, 046610 (2005).
 - ¹²G. V. Eleftheriades, A. K. Iyer, and P. C. Kremer, *IEEE Trans. Microwave Theory Tech.* **50**, 2702 (2002).
 - ¹³A. Lai, T. Itoh, and C. Caloz, *IEEE Microw. Mag.* **5**, 34 (2004).
 - ¹⁴C. Caroz and T. Itoh, *IEEE Trans. Antennas Propag.* **52**, 1159 (2004).
 - ¹⁵Yi-Jang Hsu, Yen-Chun Huang, Jiann-Shing Lih, and Jyh-Long Chern, *J. Appl. Phys.* **96**, 1979 (2004).
 - ¹⁶J. D. Baena, R. Marqués, F. Medina, and J. Martel, *Phys. Rev. B* **69**, 014402 (2004).
 - ¹⁷G. V. Eleftheriades and O. F. Siddiqui, *IEEE Trans. Microwave Theory Tech.* **53**, 396 (2005).
 - ¹⁸M. Ö. Oktel and Ö. E. Müstecaplıoğlu, *Phys. Rev. A* **70**, 053806 (2004).
 - ¹⁹C. G. Parazzoli, R. B. Gregor, K. Li, B. E. C. Koltenbah, and M. Tanielian, *Phys. Rev. Lett.* **90**, 107401 (2003).
 - ²⁰A. Berrier, M. Mulot, M. Swillo, M. Qiu, L. Thylen, A. Talneau, and S. Anand, *Phys. Rev. Lett.* **93**, 073902 (2004).
 - ²¹V. M. Agranovich, Yu. N. Gartstein, and A. A. Zakhidov, *Phys. Rev. B* **73**, 045114 (2006).
 - ²²C. W. Qiu, L. W. Li, H. Y. Yao, and S. Zouhdi, *Phys. Rev. B* **74**, 115110 (2006).
 - ²³C. W. Qiu, H. Y. Yao, S. Zouhdi, L. W. Li, and M. S. Leong, *Microwave Opt. Technol. Lett.* **48**, 2534 (2006).
 - ²⁴I. V. Lindell, A. H. Sihvola, S. A. Tretyakov, and A. J. Viitanen, *Electromagnetic Waves in Chiral and Bi-Isotropic Media* (Artech House, Boston, 1994).
 - ²⁵S. Tretyakov, I. Nefedov, A. Sihvola, S. Maslovski, and C. Simovski, *J. Electromagn. Waves Appl.* **17**, 695 (2003).
 - ²⁶J. B. Pendry, *Science* **306**, 1353 (2004).
 - ²⁷H. Dakhcha, O. Ouchetto, and S. Zouhdi, in *Proceedings of Bi-anisotropics 2004* (unpublished), p. 132.
 - ²⁸N. Engheta, D. L. Jaggard, and M. W. Kowarz, *IEEE Trans. Antennas Propag.* **40**, 367 (1992).
 - ²⁹L. D. Landau and E. M. Lifshitz, *Electrodynamics of Continuous Media*, 2nd ed. (Pergamon Press, Oxford 1984).
 - ³⁰J. Q. Shen and S. He, *J. Phys. A* **39**, 457 (2006).
 - ³¹A. Lakhtakia, *Beltrami Fields in Chiral Media* (World Scientific, Singapore, 1994).
 - ³²C. H. Papas, *Theory of Electromagnetic Wave Propagation* (McGraw-Hill, New York, 1965).
 - ³³A. Ishimaru, *Electromagnetic Wave Propagation, Radiation, and Scattering* (Prentice-Hall, Englewood Cliffs, NJ, 1991).
 - ³⁴F. Jonsson and C. Flytzanis, *J. Opt. A, Pure Appl. Opt.* **2**, 299 (2000).